

# Ivermectin-Loaded Oral Microemulsion for Oral Use

Rajashree Hirlekar <sup>1,\*</sup> , Mangal Nagarsenker <sup>1</sup>, Komal Chandra <sup>1</sup>

<sup>1</sup> Department of Pharmaceutics, Vivekanand Education Society's College of Pharmacy, Affiliated to University of Mumbai, Mumbai 400 074, Maharashtra, India

\* Correspondence: [rajashree.hirlekar@ves.ac.in](mailto:rajashree.hirlekar@ves.ac.in);

Received: 11.02.2024; Accepted: 4.01.2025; Published: 20.12.2025

**Abstract:** The oral bioavailability of marketed ivermectin (IVR) tablets is 50% compared to an oral hydroalcoholic solution. In this study, we developed an oral liquid microemulsion of IVR to improve compliance in pediatric patients. Oils, surfactants, and co-surfactants were screened and selected using solubility and emulsification tests. Using the selected oil, surfactant, and co-surfactant, a pseudo-ternary phase diagram was developed at surfactant-to-co-surfactant ratios of 1:1, 2:1, and 3:1 for the purpose of identifying the microemulsion region. The final formulation was evaluated for its physical properties, stability, and *in vitro* release. Based on the solubility studies and emulsification ability, the oil, surfactant, and co-surfactant were selected. Different regions in the pseudo-ternary diagrams were identified: phase separation region, microemulsion area, emulsion gel region, microemulsion gel, w/o macroemulsion, and o/w macroemulsion. The globule size and zeta potential of the microemulsion were  $25.01 \pm 1.13$  nm and  $-5.45 \pm 0.130$  mV, respectively. *In vitro release studies indicated 100% release after 4 h. Stability studies showed that the formulation was stable for 1 month at  $30 \pm 2^\circ\text{C}/65\%$  RH and  $40 \pm 2^\circ\text{C}/75\%$  RH. An optimized, stable IVR-loaded oil-in-water microemulsion was successfully prepared to improve the drug's solubility.*

**Keywords:** onchocerciasis; ivermectin; pseudo-ternary diagram; peroral delivery; microemulsion.

© 2025 by the authors. This article is an open-access article distributed under the terms and conditions of the Creative Commons Attribution (CC BY) license (<https://creativecommons.org/licenses/by/4.0/>), which permits unrestricted use, distribution, and reproduction in any medium, provided the original work is properly cited. The authors retain copyright of their work, and no permission is required from the authors or the publisher to reuse or distribute this article, as long as proper attribution is given to the original source.

## 1. Introduction

Onchocerciasis, also known as 'river blindness', is a disease caused by the nematode *Onchocerca volvulus*, which spreads to humans through blackflies that act as vectors for the parasite [1-3]. When the mature worms start producing microfilariae (MF) one to three years after infection, onchocerciasis starts to show clinical symptoms. Acute papular onchodermatitis (APOD) and chronic papular onchodermatitis (CPOD) lesions are caused by host inflammatory responses to dead microfilariae in the tissue [4]. Active MF can enter the cornea, and if it persists there, the cornea eventually becomes opaque, turning white and hard (sclerosing keratitis), which can result in blindness [5,6]. The treatment regimen for onchocerciasis includes oral IVR tablets. IVR is a semi-synthetic anti-parasitic agent discovered in 1980 that is obtained from the bacteria *Streptomyces avermitilis* [6,7]. IVR has a high affinity for binding to glutamate-gated chloride ion channels in the nerve and muscle cells of invertebrates, which is thought to be the primary cause of its anti-parasitic effectiveness.

The pharyngeal pump, in particular, is paralyzed as a result of the opening of these chloride ion channels, which causes a gradual and irreversible increase in membrane conductance, leading to paralysis and the death of the parasite [8-10]. IVR is practically

insoluble in water, has a molecular weight of 875 g/mol, and is a lipophilic molecule with a log P value of 4.4 [10-12]. The bioavailability of the marketed tablets is 50% compared with an oral hydroalcoholic solution [6,13]. The oral bioavailability of the drug can be increased by increasing its solubility. The pediatric population has a particularly difficult time swallowing tablets and capsules [14,15]. Also, due to the discomfort and pain accompanied by intravenous administration, they naturally reject injections, affecting patient compliance. Most children's medications are available in solution, emulsion, or suspension form, as these are easier for kids to swallow. Solutions are the most popular and convenient dosage form, especially for children, as opposed to tablets and capsules [16]. The oral route is the only approved route of administration for IVR in humans for the treatment of onchocerciasis [17].

The solubility of IVR can be enhanced by administering the drug in a microemulsion. Microemulsions are isotropic, thermodynamically stable, transparent emulsions consisting of oil, surfactant, and co-surfactant, with particle sizes ranging from 20 to 200 nm. These systems can be used to deliver poorly aqueous-soluble drugs by incorporating them into the oily phase. Certain components of microemulsions have been shown to inhibit P-glycoprotein (P-gp)-mediated efflux, which helps improve the concentration of the drug in plasma [18,19, 20]. Thus, microemulsions are excellent candidates for delivering poorly water-soluble drugs.

The objective of this study was to incorporate IVR into a stable microemulsion system and evaluate it for its appearance, globule size, dilution potential, drug content, and other characteristics. The composition of the microemulsion was determined by systematically conducting solubility and transmission studies using various oils, surfactants, and co-surfactants. Release and stability studies of the optimized microemulsion were performed to investigate its performance and stability.

## 2. Materials and Methods

IVR IP (Assay 98.60 %; specific rotation -18.8) was generously supplied by Karunesh Remedies, Ankleshwar, Gujarat, as a gift sample. Stelliesters MCT 55/45 (Medium-chain triglycerides), Stelliesters OLGA (Polyoxylglycerides/ and macrogol glycerides), Dubcare GPE M, and Dubcare GPE 810 (PEG-8 caprylic and capric glycerides) were supplied by Arihant Innochem, Mumbai, India. Miglyol 812 N (Medium-chain triglycerides) was obtained from IOI Chemical. Labrafac™ Lipophile WL 1349 (Medium-chain triglycerides), Lauroglycol™ 90 (Propylene glycol monolaurate (type II)), Transcutol® HP (Diethylene glycol monoethyl ether), and Capryol® 90 (Propylene glycol monocaprylate) were supplied by Gattefosse, India. Kolliphor® PS 80 (Polysorbate 80/Tween 80), Kolliphor® RH 40 (Polyoxyl 40 Hydrogenated Castor Oil), and Kolliphor® ELP (PEG-35 Castor Oil) were procured from BASF, India, as gift samples. All additional chemicals and reagents required for the study were of analytical grade. Millipore water was used to prepare the microemulsion.

### 2.1. Preliminary screening of excipients.

#### 2.1.1. Solubility studies.

In accordance with earlier reports, with certain modifications, the drug's solubility was determined in a range of oils, surfactants, and co-surfactants. Briefly, the excess drug was added to the oil, surfactant, or co-surfactant in a vial and incubated in a shaker incubator at 200 rpm and 25 °C for 48 hours. After 48 h, the vials were removed, and the drug-excipient mixture was centrifuged in Eppendorf tubes at 5000 rpm for 15 minutes. The filtered supernatant was

diluted with methanol and analyzed for drug concentration using a UV–visible spectrophotometer (Shimadzu UV-1800) at 245 nm. The drug concentration in the supernatant was determined using an appropriate blank solution to avoid interference from excipients on absorbance.

#### 2.1.2. Transmittance studies.

*Emulsification ability of the surfactant:* The surfactant's emulsification ability was determined by adding 300 mg of oil to 300 mg of surfactant. Then, the mixture was vortexed, followed by heating at 45°C to obtain an isotropic mixture. 50 mg of the mixture was diluted with 50 mL of distilled water. This mixture was then allowed to stand for 2 h, after which the transmittance was measured against distilled water as a blank at 638.2 nm using a UV-visible spectrophotometer (Shimadzu UV-1800) [21].

*Emulsification ability of co-surfactant:* This study was performed with some modifications to the previously reported method [22]. The emulsification ability of the co-surfactant was determined by adding a known amount of co-surfactant to a fixed amount of surfactant. A fixed amount of oil was added to this mixture. Then, the mixture was vortexed, followed by heating at 45°C to obtain an isotropic mixture. From the mixture, 50 mg was diluted with water to form a fine emulsion. This emulsion was then allowed to stand for 2 h, after which the transmittance was measured at 638.2 nm against water as a blank using a UV-visible spectrophotometer (Shimadzu UV-1800).

#### 2.1.3. Construction of pseudo-ternary phase diagram.

Blank and drug-loaded pseudo-ternary phase diagrams were constructed. Based on the preliminary screening of excipients, oil, surfactant, and co-surfactant were selected. Mixtures of surfactant and co-surfactant at fixed weight ratios of 1:1, 2:1, and 3:1 were then prepared using a vortex mixer. A pseudo-ternary phase diagram was constructed with  $S_{\text{mix}}$  ratios of 1:1, 2:1, and 3:1. For each phase diagram, the ratio of oil to  $S_{\text{mix}}$  was varied as 0.5:9.5, 1:9, 1.5:8.5, 2:8, 2.5:7.5, 3:7, 3.5:6.5, 4:6, 4.5:5.5, 5:5, 5.5:4.5, 6:4, 6.5:3.5, 7:3, 7.5:2.5, 8:2, 8.5:1.5, 9:1, 9.5:0.5. The oil and  $S_{\text{mix}}$  mixture was mixed using a vortex mixture. Then water was added dropwise to each mixture, and after each drop, the mixture was vortexed and set aside. After equilibrium, the samples were visually assessed for phase separation, transparency, or turbidity, and then assigned to phase separation, clear microemulsion, macroemulsion, clear gel, or opaque gel. Water was added continuously until a change from a clear to a turbid mixture was observed. Based on weight percentage, the compositions of oil,  $S_{\text{mix}}$ , and water were determined, and the corresponding phase diagrams were constructed with Triplot software.

#### 2.1.4. Optimization by random trials for selection of microemulsion formula.

Random points were selected from the oil-in-water microemulsion region of the pseudo-ternary diagram to assess reproducibility and select the best formulation. The trial formulations were then analyzed.

#### 2.1.5. Method for preparation of microemulsion.

The drug was added to the oil and  $S_{\text{mix}}$  mixture and mixed using a vortex mixer for about 5 min, then kept for sonication until the drug completely dissolved in the mixture. A

fixed amount of water was added to the mixture, which was then vortexed to obtain a clear, transparent microemulsion.

## 2.2. Evaluation of microemulsion.

### 2.2.1. Appearance and transparency.

The formulations prepared were evaluated through visual observation against visible light and inspected for any precipitate or phase separation. To demonstrate the formulation's transparency, the percentage of light transmitted through the formulation was measured using a UV-visible spectrophotometer (Shimadzu UV-1800). The % transmittance was measured at 638.2 nm by keeping a double-distilled water blank.

### 2.2.2. Globule size determination.

For the analysis of globule size and PDI (polydispersity index) of the formulation, 1 mL of the sample was diluted to 10 mL with the external phase, i.e., Millipore water, before the measurement. The globule size analysis was performed using the Malvern Zetasizer Nano-ZS90 instrument.

### 2.2.3. Zeta potential.

For the measurement of zeta potential, the sample was prepared in the same manner as for globule size analysis. This test was performed using a Malvern Zetasizer Nano-ZS90 instrument.

### 2.2.4. Physical stability.

*Effect of centrifugation:* The microemulsion was centrifuged at 15000 rpm for 30 min to determine the phase behavior of the particles under gravity. The formulations were observed for any phase separation or precipitation. This method is a type of accelerated stability test and confirms the systems as microemulsions [23].

*Dilution potential:* The microemulsion prepared was diluted 1000 times with an external phase (water). The diluted formulation was observed for any phase separation or precipitation. The transparency of the diluted formulation was also checked by performing the transmittance study. The particle size and PDI of the diluted formulations were measured using the Malvern Zetasizer Nano-ZS90 instrument [24].

*Heating-cooling cycle:* The formulation was stored at 45°C and 4°C for 48 h each and then evaluated for particle size and PDI. The formulation was also checked for any signs of phase separation, precipitation, or changes in transparency [21].

### 2.2.5. pH of the formulation.

The pH of the microemulsion formulation was measured using a digital pH meter (DBK Instruments).

### 2.2.6. Drug content.

A suitable amount of the formulation equivalent to 3 mg of the drug was weighed, diluted to 10 mL with methanol, and sonicated for 10 min to completely dissolve the

formulation. The diluted sample was then filtered using a syringe filter with a 0.22  $\mu\text{m}$  pore size. The same procedure was followed for blank formulations without drugs. The final sample containing the drug was analyzed using a UV spectrophotometer at 245 nm, with the formulation blank used as a reference. According to the UV absorbance, if necessary, dilutions were made further for both the sample and the blank. This experiment was performed in triplicate.

#### 2.2.7. In-vitro release study.

The *in-vitro* release study was performed using the dialysis bag (molecular weight cutoff of 12000–14000 kilodaltons) method for drug solution, drug suspension, and microemulsion formulation. A dialysis bag pre-soaked for 24 h in the release medium (sodium phosphate buffer pH 7 with 0.5% sodium lauryl sulfate) was used. The formulation-filled dialysis bag was then attached to a magnetic bead and placed in a beaker containing 150 mL of the release medium. The beaker was kept on a magnetic stirrer, and the rpm was adjusted to 50. The aliquots were withdrawn and replaced immediately with a release medium. The samples were analyzed using a UV-visible spectrophotometer, with the release medium as the blank. The percent cumulative release of the drug was calculated from the calibration curve in the release medium [25].

#### 2.2.8. Stability studies.

The final formulation, i.e., the microemulsion, was subjected to stability studies for 1 month. The final formulation was filled into glass vials, capped with rubber caps, and sealed with parafilm. Then the formulation was stored at  $30\pm 2^\circ\text{C}/ 65\% \text{ RH}$  and  $40\pm 2^\circ\text{C}/ 75\% \text{ RH}$ . The formulations were evaluated for their color, transparency, pH, particle size, PDI, zeta potential, and drug content at 0, 15, and 30 d.

### 3. Results and Discussion

#### 3.1. Preliminary screening of excipients.

##### 3.1.1. Solubility studies.

Screening of different oils, surfactants, and co-surfactants was performed to select the most suitable excipients. The drug's solubility in various oils is shown in Figure 1a. To prevent drug precipitation from the formulation, the oil with the highest solubilizing capacity should be selected. The drug's highest solubility was observed in oleic acid compared to other oils. The main difference among excipients lies in their carbon chain lengths and functional groups (acid vs. ester), with oleic acid and ethyl oleate being long-chain and unsaturated, while Labrafac™ Lipophile WL 1349, Stelliesters MCT 55/45, and Miglyol 812 N are mixtures of medium-chain, saturated fatty acids and triglycerides. The probable reason for the solubilization mechanism is that lipophilic molecules and BCS class-II molecules generally exhibit higher solubility in long-chain triglycerides (LCTs) compared to medium-chain triglycerides (MCTs), as the longer chains in LCTs provide a more favorable environment for dissolving large, non-polar molecules. However, MCTs are still useful, especially when faster drug absorption or bioavailability is desired. But oleic acid is a long-chain fatty acid, so it would be difficult to emulsify it in comparison to other oils, and it is also an unsaturated fatty acid, increasing the risk of oxidation [26-28]. So, Stelliesters MCT 55/45 was selected as the

oil phase. The solubility of drugs in the oils screened was found to be in the following order: oleic acid > Stelliesters MCT 55/45 > Labrafac<sup>TM</sup> Lipophile WL 1349 > Miglyol 812 N > Ethyl oleate. Figure 1b illustrates the solubility of the drug in different surfactants and co-surfactants. Among the surfactants, Kolliphor® PS 80 showed the highest solubility. The order of solubility of drugs in surfactants was found to be Kolliphor® PS 80 > Dubcare GPE 810 > Kolliphor® RH 40 > Stelliesters OLGA > Dubcare GPE M > Kolliphor® ELP. In the case of the co-surfactant, Capryol® 90 had the highest solubility. The order of solubility of the drug in co-surfactants was found to be Capryol® 90 > Transcutol® HP > Lauroglycol<sup>TM</sup> 90.

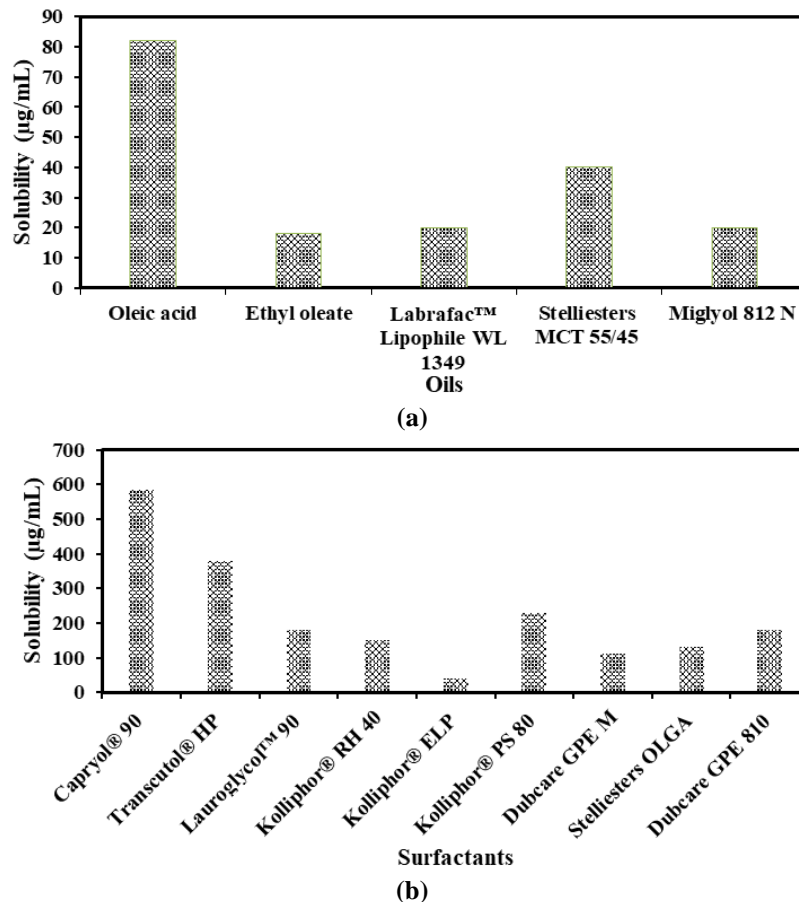


**Figure 1.** Solubility of drug in (a) oil; (b) surfactants and co-surfactants.

### 3.1.2. Transmittance studies.

*Emulsification ability of surfactant:* The results of the emulsification ability of the various surfactants with the selected oil, Stelliesters MCT 55/45, are given in Table 1. From the emulsification study of the surfactant with the selected oil, it was noted that Kolliphor® RH 40 showed the highest transmittance when compared to the other surfactants. So, Kolliphor® RH 40 was selected as the surfactant.

**Table 1.** Emulsification ability of surfactant.

Surfactant	% Transmittance
Dubcare GPE 810	76.4
Stelliesters OLGA	7.2
Dubcare GPE M	44.4
Kolliphor® PS 80	18.5
Kolliphor® ELP	88.5
Kolliphor® RH 40	93.5

**Emulsification ability of co-surfactant:** The results of the emulsification ability of the various co-surfactants with the selected oils, Stelliesters MCT 55/45 and Kolliphor® RH 40, are given in Table 2. From the emulsification study of the co-surfactant with the selected oil and surfactant, it was noted that Capryol® 90 showed the highest transmittance when compared to the other surfactants. So Capryol® 90 was selected as the co-surfactant.

**Table 2.** Emulsification ability of co-surfactants.

Oil: S <sub>mix</sub>	Surfactant: Co-surfactant	Co-surfactant	% Transmittance
1:1	1:1	Capryol® 90	78.9
1:1	1:1	Transcutol® HP	31.4
1:1	1:1	Lauroglycol™ 90	Hazy
1:2	1:1	Capryol® 90	92.7
1:2	1:1	Transcutol® HP	Hazy
1:2	1:1	Lauroglycol™ 90	Hazy
1:2	2:1	Capryol® 90	99.8
1:2	2:1	Transcutol® HP	Hazy
1:2	2:1	Lauroglycol™ 90	93.7

**3.2. Construction of pseudo-ternary phase diagram.**

The pseudo-ternary phase diagrams were constructed using Stelliesters MCT 55/45, Kolliphor® RH 40, and Capryol® 90 as oil phase, surfactant, and co-surfactant, respectively. Three different ratios of surfactant—co-surfactant (S<sub>mix</sub>)—were utilized to see their impact on the microemulsion region. The ternary phase diagrams for S<sub>mix</sub> ratios 1:1, 2:1, and 3:1 were plotted using the triplot software, as represented in Figure 2. Different regions were obtained during the construction of the pseudo-ternary diagram, which is somewhat similar to previously reported literature [29,30]. The color coding for different areas in the pseudo-ternary diagram is as follows: the grey region represents the phase separation (PS) region, the sky blue region represents the oil in the water microemulsion area (o/w ME), the orange region represents the water in oil microemulsion area (w/o ME), the yellow region represents the emulsion gel (EM gel) region, the green region represents the water in oil macroemulsion (w/o EM), and the pink region represents the oil in water macroemulsion (o/w EM).

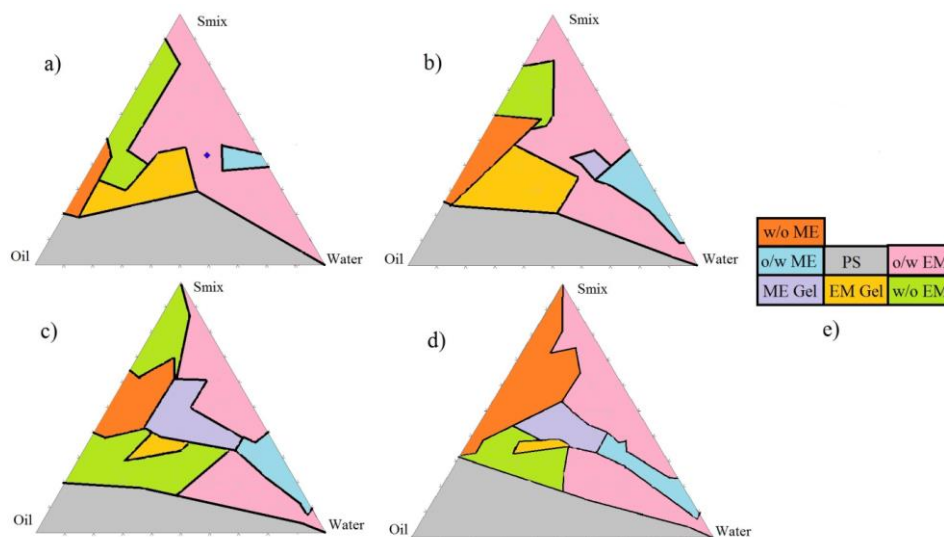


**Figure 2.** (a) Blank pseudo-ternary diagram with S<sub>mix</sub> 1:1; (b) Blank pseudo-ternary diagram with S<sub>mix</sub> 2:1; (c) Blank pseudo-ternary diagram with S<sub>mix</sub> 3:1; (d) Drug loaded pseudo-ternary diagram with S<sub>mix</sub> 3:1; (e) Color coding for different regions in pseudo-ternary diagram; o/w ME: oil in water microemulsion, w/o ME: water in oil microemulsion, PS: Phase Separation, ME Gel: Microemulsion Gel, EM Gel: Emulsion gel, o/w EM: oil in water Emulsion, w/o EM: water in oil emulsion

There was an increase in the microemulsion area (both o/w and w/o) when the  $S_{mix}$  ratio was increased from 1:1 to 3:1. Thus, the largest microemulsion region was obtained with a  $S_{mix}$  ratio of 3:1. The result of the blank microemulsion indicated that the  $S_{mix}$  ratio of 3:1 is optimal for the selected oil phase, so this  $S_{mix}$  ratio was used for the formulation of the microemulsion. The microemulsion area remained almost unchanged after the drug was incorporated.

### 3.3. Optimization by random trials for selection of the best microemulsion formula.

The optimum concentrations of oil,  $S_{mix}$  mixture, and water were determined based on appearance, particle size, PDI, and % transmittance, as shown in Table 3. All formulations were transparent and had good particle size and PDI. As we planned to make an oral liquid formulation, the F1 formula was rejected because of its high viscosity. Formulations F2, F3, and F4 were also rejected due to their lower transmittance. Formulation F5 showed higher % transmittance than F2, F3, and F4 and also possessed optimal consistency, desirable for oral liquid formulations. So, based on these results, formulation F5 was selected as the best formula. Also, it is desirable to keep the surfactant concentration as low as possible so that the F5 formulation satisfies all the desired characteristics.

**Table 3.** Random formulation trials in the o/w microemulsion region.

Formulation Code	% Oil	% $S_{mix}$	% Water
F1	10	40	50
F2	15	30	55
F3	12	23	65
F4	10	20	70
F5	5	20	75

### 3.4. Evaluation of microemulsion.

The appearance of all the formulations was clear and transparent in nature, with a slight bluish tinge, among which F5 showed the highest percentage transmittance of  $95.9 \pm 0.9$ , as mentioned in Table 4. As Lei He mentioned previously, microemulsions can impart a bluish tinge to the formulation [30]. The average globule size and PDI of all formulations were below 50 nm and 0.2, respectively, as shown in Table 4. An ideal microemulsion typically aims for a refractive index intermediate between those of oil and water to maintain stability and clarity. This often leads to a refractive index in the range of 1.35 to 1.5. All the results obtained are within the range.

**Table 4.** Evaluation of random formulation trials.

Code	Oil (%)	$S_{mix}$ (%)	Water (%)	Appearance	Refractive index	Average particle size (nm)	PDI	% Transmittance
F 1	10	40	50	Clear viscous liquid	$1.3945 \pm 0.002$	$26.03 \pm 1.45$	$0.187 \pm 0.04$	$93.8 \pm 0.9$
F 2	15	30	55	Bluish transparent liquid	$1.389 \pm 0.002$	$35.01 \pm 2.02$	$0.073 \pm 0.01$	$82.2 \pm 1.1$
F 3	12	23	65	Bluish transparent liquid	$1.3765 \pm 0.001$	$37.53 \pm 1.62$	$0.088 \pm 0.02$	$81.8 \pm 1.2$
F 4	10	20	70	Bluish transparent liquid	$1.365 \pm 0.001$	$35.81 \pm 1.20$	$0.076 \pm 0.02$	$88.4 \pm 0.7$

Code	Oil (%)	S <sub>mix</sub> (%)	Water (%)	Appearance	Refractive index	Average particle size (nm)	PDI	% Transmittance
F5	5	20	75	Bluish transparent liquid	1.363 ± 0.000	25.01 ± 1.13	0.082 ± 0.01	95.9 ± 0.9

The microemulsion was analyzed for its surface potential at 25°C. The microemulsion had a zeta potential of  $-5.45 \pm 0.130$  mV. The surface charge helps disperse the small particles of the microemulsion in the continuous phase. The electric potential at the boundary of the double layer is known as the zeta potential of the particles and typically ranges from +100 mV to -100 mV. The magnitude of the zeta potential is predictive of colloidal stability. Microemulsions with zeta potential values greater than +25 mV or less than -25 mV typically have high degrees of stability. Because the microemulsion components are non-ionic, the charge was found to be close to zero. Such microemulsions are stabilized by dipole and hydrogen bond interactions between the non-ionic surfactant and the hydration layer of water on the hydrophilic surface of the surfactant. Non-ionic surfactants do not ionize in aqueous solutions because their hydrophilic groups are non-dissociable. Microemulsions can be stable even with low zeta potentials, particularly when they possess favorable interfacial properties, small droplet sizes, and optimal formulation conditions [31-33].

The physical stability of the formulations was determined by subjecting them to centrifugation, heating, cooling cycles, and dilution tests. After centrifugation, no precipitation or phase separation was observed in the formulation, indicating that it was stable, as evidenced by the values in Table 5. After the heating and cooling cycles, there was no sign of precipitation, phase separation, or change in transparency, and the particle size and PDI of the formulation were found to be  $22.60 \pm 1.14$  nm and  $0.160 \pm 0.02$  nm, respectively. Except for F5, all formulations experienced physical instability during the first 48 hours of storage; therefore, analysis was not performed for these formulations. From the dilution test, it was observed that all formulations except F4 had 1,000 times the dilution potential, whereas the F4 formulation showed a significant increase in PDI upon dilution, which could indicate drug precipitation. The percent transmittance increased with dilution; no phase separation was observed until 1,000 dilutions (Table 6). The pH of the microemulsion was  $4.6 \pm 0.21$ , within the acceptable range for oral formulations [34]. The drug content of formulation F5 was  $98.5 \pm 0.8\%$ . On the basis of the previous tests, the F5 formulation was selected for further evaluation.

**Table 5.** Effect of centrifugation on formulation.

Parameters	Before centrifugation	After centrifugation
Observation	Clear transparent	Clear, transparent, and no phase separation
Particle size (nm)	25.01 ± 1.13	24.26 ± 1.62
PDI	0.082 ± 0.01	0.08 ± 0.02

**Table 6.** Effect of dilution on formulations.

Code	Particle size (nm)			PDI			% Transmittance			
	Dilution	10x	100x	1000x	10x	100x	1000x	10x	100x	1000x
F1		26.03	28.06	30.04	0.187	0.081	0.178	93.8	95.3	98.5
F2		35.01	35.11	36.54	0.073	0.057	0.193	82.2	95.6	99.2
F3		37.53	38.26	39.73	0.088	0.127	0.204	81.8	95.6	97.5
F4		35.81	37.26	53.48	0.076	0.159	0.497	88.4	95.2	97.3
F5		24.54	24.81	38.50	0.082	0.145	0.196	95.9	99.5	99.9

### 3.4.1. In-vitro drug release study from microemulsion.

Figure 3 shows the comparative *in vitro drug release from the* F5 microemulsion (ME), IVR suspension, and IVR solution. It was observed that at the end of 4 hr, the F5 microemulsion (ME) and the drug solution had 100% release, whereas the drug suspension showed only 34.10% release. Even though the drug is insoluble in water, it showed some release in the medium, which was due to the SLS present in the release medium. The order of drug release was: drug solution > F5 microemulsion > drug suspension.

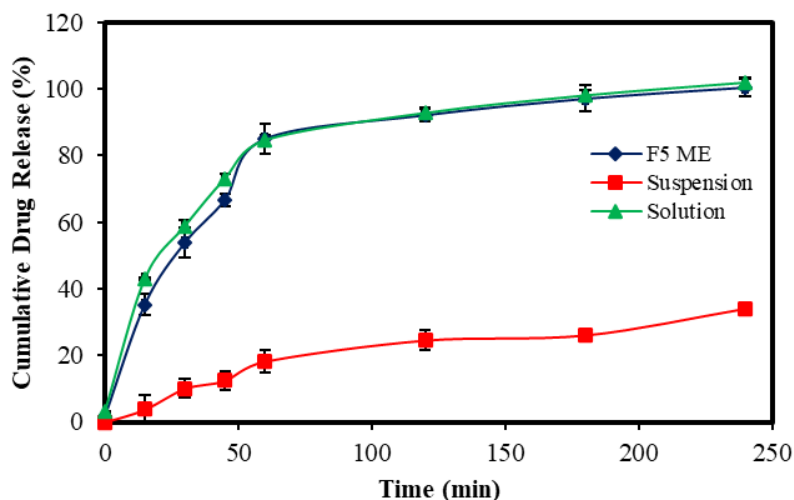


Figure 3. Comparative *in-vitro* drug release study of F5 microemulsion (ME), IVR suspension, and IVR solution.

### 3.4.2. Stability study.

Table 7 shows the results of the evaluation parameters for samples kept at  $30 \pm 2^\circ\text{C}/65\%$  % RH and  $40^\circ\text{C}/75\%$  RH, respectively, at 0, 15, and 30 days during stability studies. The formulation was stable for the duration of 30 d.

**Table 7.** Stability study results.

Period	Color	Transparency	pH	Particle size (nm)	PDI	Zeta Potential (mV)	Drug content (%)
$30 \pm 2^\circ\text{C}/65\%$ RH							
0 d	Bluish	Transparent	4.8	$25.01 \pm 1.13$	$0.082 \pm 0.01$	$-5.45 \pm 0.130$	$98.5 \pm 0.8$
15 d	Bluish	Transparent	4.78	$24.95 \pm 1.82$	$0.102 \pm 0.01$	$-4.52 \pm 0.120$	$99.3 \pm 0.4$
30 d	Bluish	Transparent	4.62	$25.62 \pm 1.52$	$0.097 \pm 0.01$	$-6.22 \pm 0.162$	$97.02 \pm 0.7$
$40 \pm 2^\circ\text{C}/75\%$ RH							
0 d	Bluish	Transparent	4.75	$25.01 \pm 1.13$	$0.082 \pm 0.01$	$-5.45 \pm 0.130$	$98.5 \pm 0.8$
15 d	Bluish	Transparent	4.67	$26.85 \pm 1.13$	$0.080 \pm 0.01$	$-5.82 \pm 0.108$	$100.06 \pm 0.8$
30 d	Bluish	Transparent	4.63	$27.53 \pm 1.13$	$0.124 \pm 0.01$	$-4.62 \pm 0.176$	$98.85 \pm 0.10$

## 4. Conclusions

An optimized, stable IVR-loaded oil-in-water microemulsion was successfully prepared to improve the drug's solubility. An attempt was made to prepare a microemulsion using Stelliesters MCT 55/45 as the oil phase. Different regions were identified during construction of the pseudo-ternary phase diagram, showing changes in phase behavior with composition. The optimized formula consisted of 5% oil (Stelliesters MCT 55/45), 20% Smix

(a mixture of Kolliphor® RH 40 and Capryol® 90), and 75% water. The globule size of the formulation was within the range of the IUPAC definition of microemulsion. The formulation exhibited faster release than a suspension, indicating increased drug solubility, which might also increase its bioavailability.

### **Author Contributions**

Conceptualization, R.H. and M.N.; methodology, R.H.; software, K.C.; validation, R.H., M.N., and K.C.; formal analysis, K.C.; investigation, K.C.; resources, R.H.; data curation, K.C.; writing—original draft preparation, K.C.; writing—review and editing, R.H.; visualization, K.C.; supervision, R.H. and M.N.; project administration, R.H.; funding acquisition, R.H. All authors have read and agreed to the published version of the manuscript.

### **Institutional Review Board Statement**

Not applicable.

### **Informed Consent Statement**

Not applicable.

### **Data Availability Statement**

Data supporting the findings of this study are available upon reasonable request from the corresponding author.

### **Funding**

This research received no external funding.

### **Acknowledgments**

We are grateful towards Dr. Mangal Nagarsenker (Professor Emeritus, Bombay College of Pharmacy, Mumbai, India; Research Advisor, Vivekanand Education Society's College of Pharmacy, Chembur, Mumbai, India) for providing eminent insights for this research. Additionally, we would like to express our gratitude to Dr. Sameer Padhye (Deputy Manager, Technical Services (Pharma), Arihant Innochem Pvt. Ltd. India) for providing excipients.

### **Conflicts of Interest**

The authors declare no conflict of interest.

### **References**

1. Benjamin, G.; Lara, P.; Laura, N. Onchocerciasis identified with anterior segment ocular examination and FDG-PET/CT imaging. *Clin Infect Pract* **2025**, 100511. <https://doi.org/10.1016/j.clinpr.2025.100511>.
2. World Health Organization (WHO). Onchocerciasis Key Fact (Geneva) (2022). Available online: <https://www.who.int/news-room/fact-sheets/detail/onchocerciasis> (accessed on 03 June 2024).
3. Timothy, J. Niger eliminates onchocerciasis. *Lancet* **2025**, 25, E204-209. [https://doi.org/10.1016/S1473-3099\(25\)00173-2](https://doi.org/10.1016/S1473-3099(25)00173-2).
4. Hong, A.R.; Opoku, N.O.; Weil, G.J.; Kanza, E.M.; Gyasi, M.E. New Research Aims to Optimize Therapy Against Onchocerciasis. *Mo Med*. **2022**, 119, 55-59.

5. Timothy, J. A new key-player for onchocerciasis elimination. *Lancet* **2023**, *23*, 413-419, [https://doi.org/10.1016/S1473-3099\(23\)00151-2](https://doi.org/10.1016/S1473-3099(23)00151-2).
6. STROMEKTOL ivermectin 3mg tablet blister pack (181338). Available online: <https://www.tga.gov.au/resources/artg/181338> (accessed on 03 November **2023**).
7. Mark, D.K.; Jennifer, D.N.; Timothy, G.G.; Robin, N.B. Structural mechanism underlying the differential effects of ivermectin and moxidectin on the *C. elegans* glutamate-gated chloride channel GLC-2. *Biomed. Pharmacother.* **2022**, *145*, 112380, <https://doi.org/10.1016/j.biopha.2021.112380>.
8. Nabi, M.; Mohebi, F.; Zalpoor, H.; Aziziyan, F.; Akbari, A.; Moradi-Sardareh, H.; Bahreini, E.; Moeini, A.M.; Effatpanah, H. A cellular and molecular biology-based update for ivermectin against COVID-19: is it effective or non-effective? *Inflammopharmacology* **2023**, *31*, 21-35, <https://doi.org/10.1007/s10787-022-01129-1>.
9. Ragó, Z.; Tóth, B.; Szalenko-Tóké, Á.; Bella, Z.; Dembrovszky, F.; Farkas, N. Results of a systematic review and meta-analysis of early studies on ivermectin in SARS-CoV-2 infection. *Geroscience* **2023**, *45*, 2179-2193, <https://doi.org/10.1007/s11357-023-00756-y>.
10. Reis, G.; Silva, E.; Thabane, L.; Milagres, A.C. Effect of Early Treatment with Ivermectin among Patients with Covid-19. *N. Engl. J. Med.* **2022**, *386*, 1721-1731, <https://doi.org/10.1056/NEJMoa2115869>.
11. Vasanti, S. Ivermectin: A Critical Review on Characteristics, Properties, and Analytical Methods. *J. AOAC Int.* **2023**, *106*, 534-557, <https://doi.org/10.1093/jaoacint/qsad031>.
12. Marcolino, M.S.; Meira, K.C.; Guimarães, N.S.; Motta, P.P.; Chagas, V.S.; Kelles, S.M.B.; Valacio, R.A.; Ziegelmann, P.K. Systematic review and meta-analysis of ivermectin for treatment of COVID-19: evidence beyond the hype. *BMC Infect. Dis.* **2022**, *22*, 639-648, <https://doi.org/10.1186/s12879-022-07589-8>.
13. Soolantra (IVR) Cream, 1%. Department of Health and Human Services; Public Health service; Food and Drug Administration; Centre for Drug Evaluation and Research. Available online: [https://www.accessdata.fda.gov/drugsatfda\\_docs/nda/2014/206255Orig1s000PharmR.pdf](https://www.accessdata.fda.gov/drugsatfda_docs/nda/2014/206255Orig1s000PharmR.pdf) (accessed on 26 November **2023**).
14. Adam, M.F.; Eulambius, M.M.; Eliford, N.K.; Gerald, S.K. Pharmacokinetics of ivermectin after mass drug administration in lymphatic filariasis endemic communities of Tanzania. *CPT: PSP* **2023**, *12*, 1884-1896, <https://doi.org/10.1002/psp4.13038>.
15. Algorta, J.; Krolewiecki, A.; Pinto, F.; Gold, S.; Muñoz, J. Pharmacokinetic Characterization and Comparative Bioavailability of an Innovative Orodispersible Fixed-Dose Combination of Ivermectin and Albendazole: A Single Dose, Open Label, Sequence Randomized, Crossover Clinical Trial in Healthy Volunteers. *Front. Pharmacol.* **2022**, *13*, 914886, <https://doi.org/10.3389/fphar.2022.914886>.
16. Boateng, J. Drug Delivery Innovations to Address Global Health Challenges for Pediatric and Geriatric Populations (Through Improvements in Patient Compliance). *J. Pharm. Sci.* **2017**, *106*, 3188-3198, <https://doi.org/10.1016/j.xphs.2017.07.009>.
17. Canga, A.G.; Prieto, A.M.S.; Diez Liébana, M.J.; Martínez, N.F.; Sierra Vega, M.; García Vieitez, J.J. The Pharmacokinetics and Interactions of IVR in Humans - A Mini-Review. *AAPS J.* **2008**, *10*, 42-46, <https://doi.org/10.1208/s12248-007-9000-9>.
18. Srinivas, B.; Shruti, M.; Sameer, P. Self-microemulsifying drug delivery system as carrier for the oral delivery of glimepiride: Formulation development, optimization, in-vitro characterization, stability assessment, ex-vivo permeation, and in-vivo antidiabetic activity in albino mice. *Atlantic J Med Sci Res* **2024**, *4*, 9-18. <https://doi.org/10.5455/atjmed.2023.09.051>.
19. Khan, S.; Shyamkumar, T.S.; Aneesa, V.A.; Dhama, K.; Pawde, A.M.; Pal, A. Current Therapeutic Applications and Pharmacokinetic Modulations of IVR. *Vet. World* **2019**, *12*, 1204-1211, <https://doi.org/10.14202/vetworld.2019.1204-1211>.
20. Bhairy, S.; Momin, A.; Hirlekar, R. Assessment of ex-vivo intestinal permeability and lymphatic uptake of curcumin and piperine-loaded nanostructured lipid carriers. *German J Pharm Biomater* **2024**, *3*, 19-24. <https://doi.org/10.5530/gjpb.2024.2.6>.
21. Sharda, S.; Rohit, M. Nanoemulsion: An Emerging Novel Technology for Improving the Bioavailability of Drugs. *Scientifica* **2023**, 6640103, 1-25. <https://doi.org/10.1155/2023/6640103>.
22. Date, A.A.; Nagarsenker, M.S. Design and Evaluation of Self-Nanoemulsifying Drug Delivery Systems (SNEDDS) for Cefpodoxime Proxetil. *Int. J. Pharm.* **2007**, *329*, 166-172, <https://doi.org/10.1016/j.ijpharm.2006.08.038>.
23. Nagaveni, P.; Mounika, G.; Saravanakumar, K. A Detailed Review on Micro Emulsions. *Int J Pharm Sci* **2025**, *3*, 1272-1282. <https://doi.org/10.5281/zenodo.14670480>.

24. Aman, L.; Gayatri, K.; Vaishnavi, K. A Review on Formulation and Evaluation OF Micro-Emulsion. *Int J Pharm Sci* **2025**, *3*, 2198-205. <https://doi.org/10.5281/zenodo.15400592>.
25. Bhairy, S.; Momin, A.; Hirlekar, R. Formulation Development and Evaluation of Dry Adsorbed Nanoparticles of Curcumin and Piperine dual drug loaded Nanostructured Lipid Carriers, *Int J Pharm Sci Nanotech* **2023**, *16*, 6844-6864. <https://doi.org/10.37285/ijpsn.2023.16.4.2>.
26. Qian, J.; Meng, H.; Xin, L.; Xia, M.; Shen, H.; Li, G.; Xie, Y. Self-Nanoemulsifying Drug Delivery Systems of Myricetin: Formulation Development, Characterization, and in Vitro and in Vivo Evaluation. *Colloids Surf. B Biointerfaces* **2017**, *160*, 101-109, <https://doi.org/10.1016/j.colsurfb.2017.09.020>.
27. Leyton, J.; Drury, P.J.; Crawford, M.A. Differential Oxidation of Saturated and Unsaturated Fatty Acids in Vivo in the Rat. *Br. J. Nutr.* **1987**, *57*, 383-393, <https://doi.org/10.1079/bjn19870046>.
28. Patel, V.; Lalani, R.; Bardoliwala, D. Lipid-Based Oral Formulation Strategies for Lipophilic Drugs. *AAPS PharmSciTech* **2018**, *19*, 3609–3630, <https://doi.org/10.1208/s12249-018-1188-8>.
29. Mahdi, E.S.; Sakeena, M.H.; Abdulkarim, M.F.; Abdullah, G.Z.; Sattar, M.A.; Noor, A.M. Effect of Surfactant and Surfactant Blends on Pseudoternary Phase Diagram Behavior of Newly Synthesized Palm Kernel Oil Esters. *Drug Des. Devel. Ther.* **2011**, *5*, 311-323, <https://doi.org/10.2147/DDDT.S15698>.
30. Cavalcanti, A.L.M.; Reis, M.Y.F.A.; Silva, G.C.L.; Ramalho, Í.M.M.; Guimarães, G.P.; Silva, J.A.; Saraiva, K.L.A.; Damasceno, B.P.G.L. Microemulsion for Topical Application of Pentoxifylline: In Vitro Release and in Vivo Evaluation. *Int. J. Pharm.* **2016**, *506*, 351-360, <https://doi.org/10.1016/j.ijpharm.2016.04.065>.
31. Nawaz, H.; Bafakeeh, O.T.; Mahboob, K. Formulation and characterization of microemulsions for drug delivery. *J. Drug Deliv. Sci. Technol.* **2020**, *60*, 101992, <https://doi.org/10.1016/j.jddst.2020.101992>.
32. Ahmad, M. E.; Nagib, A. E.; Hesham, A. E. Development of Avocado oil Nanoemulsion Hydrogel using Sucrose Ester Stearate. *J Appl Pharm Sci*, **2013**, *3*, 145-147. <https://doi.org/10.7324/JAPS.2013.31226>.
33. Rajashree, H.; Alfiha, M.; Srinivas, B. Formulation development, in-vitro and ex-vivo evaluation of dry adsorbed solid lipid nanoparticles: an approach of overcoming olanzapine drawbacks. *Eur Pharm J* **2024**, *71*, 1-15. <https://doi.org/10.2478/afpuc-2024-0004>.
34. Attebäck, M.; Hedin, B.; Mattsson, S. Formulation Optimization of Extemporaneous Oral Liquids Containing Naloxone and Propranolol for Pediatric Use. *Sci. Pharm.* **2022**, *90*, 15, <https://doi.org/10.3390/scipharm90010015>.

## Publisher's Note & Disclaimer

The statements, opinions, and data presented in this publication are solely those of the individual author(s) and contributor(s) and do not necessarily reflect the views of the publisher and/or the editor(s). The publisher and/or the editor(s) disclaim any responsibility for the accuracy, completeness, or reliability of the content. Neither the publisher nor the editor(s) assume any legal liability for any errors, omissions, or consequences arising from the use of the information presented in this publication. Furthermore, the publisher and/or the editor(s) disclaim any liability for any injury, damage, or loss to persons or property that may result from the use of any ideas, methods, instructions, or products mentioned in the content. Readers are encouraged to independently verify any information before relying on it, and the publisher assumes no responsibility for any consequences arising from the use of materials contained in this publication.